First Results of ELM Triggering With a Multichamber Lithium Granule Injector Into EAST Discharges

Z. Sun, R. Lunsford, R. Maingi, J. S. Hu, D. K. Mansfield, A. Diallo, K. Tritz, J. Canik, Z. Wang, D. Andruczyk, Y. M. Wang, G. Z. Zuo, M. Huang, W. Xu, and X. C. Meng

Abstract—A critical challenge facing the basic long-pulse H-mode for ITER is to control edge-localized modes (ELMs). A new method using a multichamber lithium (Li) granule injector (LGI) for ELM triggering experiments has been developed in Experimental Advanced Superconducting Tokamak (EAST). First experimental results of the control of ELMs are obtained in EAST with a tungsten divertor. It is found that the injector has good capacities, i.e., allowing good flexibilities in granule size selection, injection rate, and injection velocity. LGI has successfully triggered ELMs during the H-mode. These results indicate the LGI would be a promising method to control ELMs in long-pulse steady-state tokamaks.

Index Terms—Edge localized modes (ELM), Experimental Advanced Superconducting Tokamak (EAST), lithium (Li) granule injection (LGI).

I. Introduction

CONTROL of edge-localized modes (ELMs) is a critical need for ITER and future devices [1], [2]. ELMs are periodic instabilities driven by excessive edge pressure gradient, edge current, or both [3]. During an ELM crash, a portion of the stored plasma energy rapidly transports to the open field lines, resulting in high heat and particle fluxes to plasma facing components (PFCs); if the heat fluxes exceed material limits, PFCs can be substantially damaged [4].

Z. Sun, Y. M. Wang, G. Z. Zuo, M. Huang, W. Xu, X. C. Meng are with the Institue of Plasma Physics, Chinese Academy of Sciences, Hefei, China.

R. Lunsford, R. Maingi, D. K. Mansfield, and A. Diallo are with Princeton Plasma Physics Laboratory, Princeton University, Princeton, NJ 08543 USA.

J. S. Hu is with the Institute of Plasma Physics, Chinese Academy of Sciences, Hefei, China, and also with the CAS key Laboratory of Photovoltaic and Energy Conservation Materials, Hefei 23031, China (e-mail: hujs@ipp.ac.cn).

K. Tritz is with Johns Hopkins University, Baltimore, MD USA.

J. Canik is with Oak Ridge National Laboratory, Oak Ridge, TN USA.

Z. Wang is with Los Alamos National Laboratory, Los Alamos, NM 87545 USA.

D. Andruczyk is with the Department of Nuclear Plasma and Radiological Engineering, Center for Plasma Material Interactions, University of Illinois at Urbana–Champaign, Urbana, IL 61801 USA.

Color versions of one or more of the figures in this paper are available online at http://ieeexplore.ieee.org.

Digital Object Identifier 10.1109/TPS.2017.2773095

Two leading methods to mitigate ELMs are to decrease ELM sizes by increasing the ELM frequency above the natural frequency [5], and to suppress ELMs altogether, e.g., with magnetic perturbations [6]. In the first technique, either fueling pellets [7]–[9] or impurity granules [10], [11] can be used. Lithium (Li) granules have shown to be effective in present day experiments, partly because of their ablation characteristics in a typical H-mode plasma [12]. However, the determination of the optimal injection characteristics (size, frequency of injection, and velocity), together with model validation and prediction for future devices, requires substantial run time. Further advances in injection technology may be able to reduce the number of the experiments required. Here, we describe a new multichamber Li granule injector (LGI) deployed on the long-pulse Experimental Advanced Superconducting Tokamak (EAST) [13], and first experimental results using the new capabilities.

II. Hardware

LGI was developed as a tool for ELMs control in the EAST plasma. These granules achieved shallow penetration and resulted in ELM triggering for granules of a sufficiently large size. An overview of LGI apparatus is briefly described here. Additional details about the setup and operation can be found in [10] and [11]. The improved apparatus employed in this paper is capable of injecting four different sizes of spherical granules which cover the range of ∼0.2–1 mm. Available velocities range from ∼30 to 110 m/s and granule injection frequencies can range from single granule injection to frequencies approaching 800 Hz for the smallest size granules (0.2–0.4 mm). The main components are as follows:

1) a four-chamber granule reservoir with a chamber selection mechanism allowing for granule size selection located above a piezoelectric dropper disk, leading granules to fall through a vertical guide tube;
2) a spinning impeller with two paddles which impact a falling granule and propel it horizontally toward the plasma edge;
3) a fast camera for monitoring the system operation and recording performance.

The schematic representation of LGI is shown in Fig. 1.

The LGI is located at the outboard midplane of EAST. The impeller axis, and thus the granule injection point, is about 2 m away from the plasma separatrix. To reduce the positional
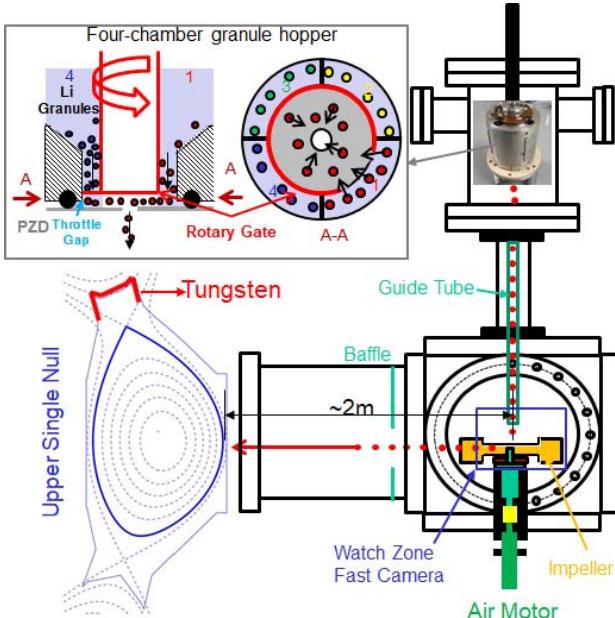
Fig. 1. Schematic of the injector hardware used in this paper. The spherical Li granules from one of four separate chambers fall through a narrow guide tube and are struck by the paddles of a rotating plastic impeller. The granules are thus horizontally redirected at higher speeds into the midplane of EAST upper single-null discharges.
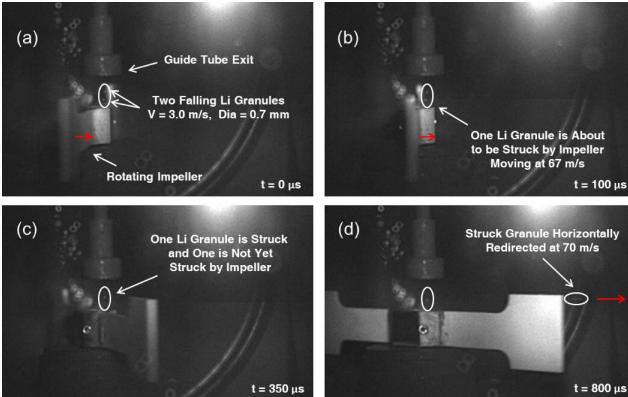

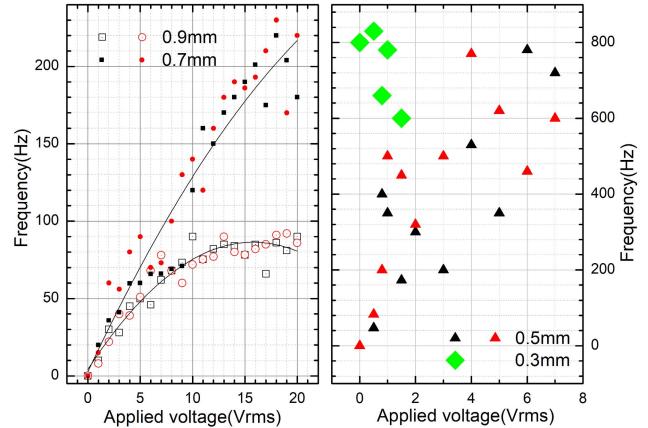Fig. 2. Four sequence images of a granule injection event.

Fig. 3. Granule drop frequencies versus applied voltage to the PZD for four separate sized granules. Drop frequency versus voltage for the larger size granules (left). and Behavior of the smaller sized granules (right).

fast camera. The video camera is set to acquire 512×384 pixel images at a 20-kHz sample rate with a 49-μs exposure time. The camera images the blue square called out in the lower right-hand side of Fig. 1, generating the images shown in Fig. 2. The images are then processed through an automated MATLAB code which extracts the granule drop frequency, granule size, impeller rotation frequency, granule velocity, ablation time, and the number ablation events from the image sequence.

Changing the size of Li granules for injection is accomplished between plasma discharges by manually advancing a rotary feed-through which supplies a feed channel to the actively selected granule chambers, as shown in the upper right-hand side of Fig. 1. For EAST experiments, the chambers were loaded with Li granules of nominal diameter 0.3, 0.5, 0.7, and 0.9 mm. The actual granule diameter in each set varies within ± 0.1 mm from the nominal diameter, set by the range of sieves used to manually sort the granules. This range of granule sizes was chosen because it spans the estimated threshold level for granule induced edge pressure perturbations which is an important variable for ELM triggering on EAST.

As shown in Fig. 1, this granule valve allows granules driven by gravity to fall onto the top of the piezoelectric disk (PZD) with a 2.5-mm central aperture. The aperture and small gap between the PZD and the bottom surface of the reservoir keeps the granules from naturally rolling to the central aperture due to the formation of bridge instabilities. When the PZD is driven into mechanical resonance by a sine-wave generator at 2.25 kHz, the spherical Li granules are compelled to fall through the aperture. The plots shown in Fig. 3 display the relationship of averaged falling frequency and the applied voltage for four nominal granule sizes. It was found that the dropping frequencies were approximately proportional to the applied voltage for the 0.9, 0.7, and 0.5-mm granules. The 0.3-mm granules could not, however, be controlled by the applied piezoelectric voltage. The 0.3-mm granules fell immediately at high frequency when the valve was rotated to the chamber because the gap is too large to inhibit-free granule flow—which was indicative of an injection gap that was too

scattering of injected granules as they cross the separatrix, the injector employs a thin guide tube to fix the position of the granule stream with respect to the impeller axis, and a rectangular injection baffle designed to reject off-normal injections. This ensures that the majority of the Li granules are launched with a predominantly horizontal injection trajectory ensuring an injection efficiency, defined as the ratio of granules successfully injected over the total number of granules dropped, of $>85\%$. As seen in Fig. 2, the granule injection events are recorded by a high-speed monochrome camera (Phantom711, by Vision Research), installed on the side of the impeller chamber. The dropped granule steam that vertically exits the guide tube is struck by rotating paddle and launched horizontally toward the discharge. As displayed in Fig. 2, this full sequence of events can be captured by the
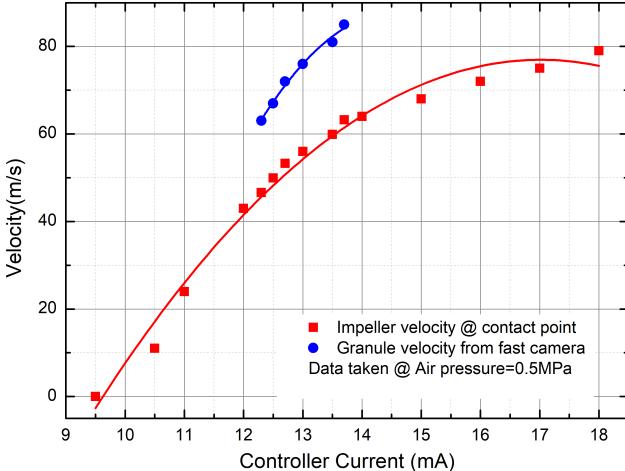
Fig. 4. Relationship among controller current, impeller velocity, and LGI velocity.

large. Also indicative of an injection gap which was too large, there was about 200-Hz scatter at same applied voltage for the 0.5-mm granules. Thus, at these lower sizes, it was more difficult to control the dropping frequency when compared to the cases of 0.7 and 0.9-mm granules. For the smaller granules, the maximum averaged frequency was higher. The maximum averaged frequency was up to 90 Hz for 0.9-mm granule and 240 Hz for 0.7-mm granule at 20 V_{rms} applied piezoelectric voltage. The range of available granule injection frequencies has been found to be suitable for effective ELM pacing experiments.

The velocity at which the granules are injected is directly proportional to the LGI impeller rotational frequency. The nominal maximum rotation frequency is 250 Hz. The relationship of granule injection velocity and the paddle rotation frequency is

$$Vg = \pi R f_p (1 + C_r)$$

where V_g is the velocity of granule; R is the distance between contact point and impeller axis, 530 mm; f_p is the rotation frequency of paddle (twice the frequency of the of impeller for the dual bladed turbine); and C_r is the coefficient of restitution. The rotation frequency is determined by the gas pressure applied to the pneumatic motor which is itself driven by an I/P transducer which responds to a controller current ranging from 4–20 mA. The calibration curve between the controller current and the impeller velocity is shown in Fig. 4. It was observed that the impeller velocity at the location of the granule contact point could be well controlled over a range from 20–80 m/s. It was also observed that the granule velocity as measured by the spatially calibrated fast camera images was 1.343–1.352 times the velocity of contact point. The coefficient of restitution for inelastic Li conditions was therefore confirmed to be ∼0.35. Thus, the granule velocity should be well controlled over the range of 27–108 m/s.

III. LI GRANULE INJECTION TRIGGERING ELM

LGI has clearly triggered ELMs during the H-mode discharge phase on EAST. Fig. 5 displays the plasma response
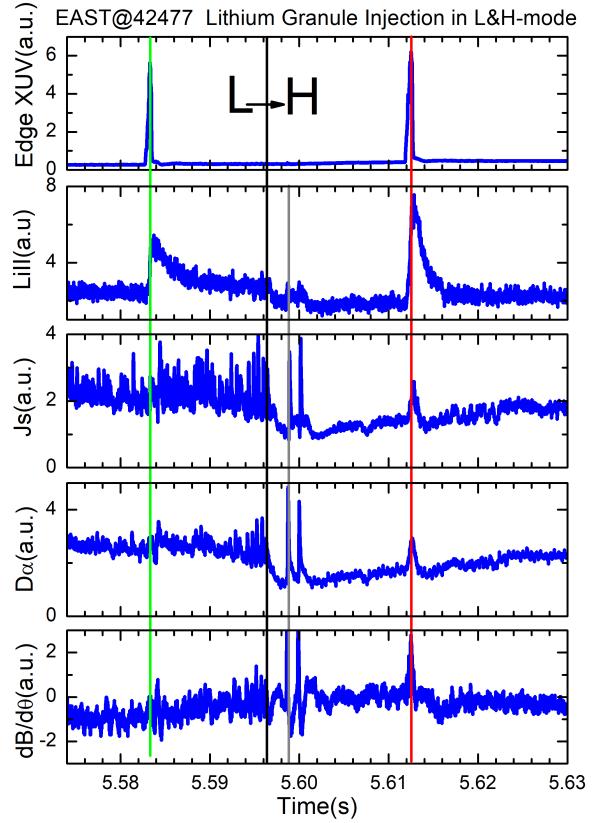

Fig. 5. Comparison of a granule injection into L- and H-mode phases of a discharge. The green line indicates the location of a granule injection into L-mode, while the red line indicates a granule injection into H-mode. The gray line is placed at the location of a natural ELM event.

when two Li granules with nominal diameter 0.7 mm and approximate velocity of 50 m/s were injected into the L-mode and H-mode phases of a single discharge as shown by the green- and red-dashed lines, respectively. Compared to LGI during the L-mode phase the diagnostic response to granule injection during the H-mode phase of the discharge can be seen in the response of the Dα emission signal as measured by a filter scope aimed at the EAST divertor, the peaked ion saturation current from the divertor Langmuir probe, and a significant magnetic perturbation from the Mirnov magnetic pickup probe. These diagnostics indicate that the efflux of particles and energy resultant from granule injection are a result of plasma response and not simply a consequence of the localized density perturbation created by the injected granule. To amplify this conclusion about granule instigated ELMs, we compare the triggered ELM denoted by the red line to a spontaneous ELM denoted by the gray line at $t = 5.598$ s, as shown in Fig. 5, the Dα, peak ion saturation current, and magnetic perturbation displayed similar behavior. Additionally, similar features can be seen when comparing the magnetic spectrum and temporal envelope from a high Nyquist frequency Mirnov magnetic pickup probe signal between a natural and a triggered ELM by a single granule injection, respectively, marked by the gray and red lines in Fig. 5. As shown in Fig. 6, there were almost the same features for frequency spectrum and envelope. The two peaks in the
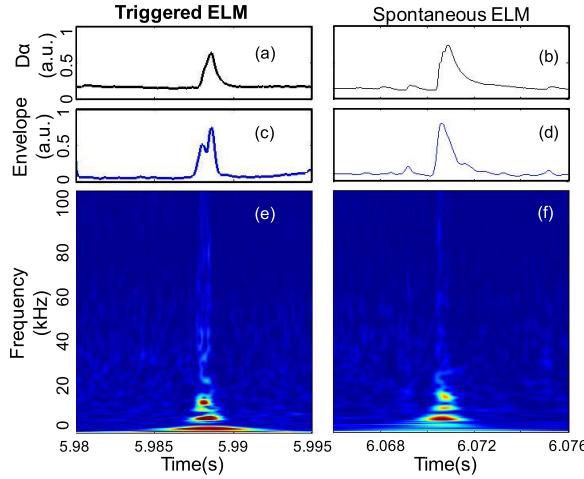
Fig. 6. Comparison of a single granule triggered and spontaneous ELM event. (a) and (b) Dα signal, (c) and (d) envelope of Minrov pickup coil signal, and (e) and (f) frequency spectrum of magnetic perturbation by wavelet transformation.
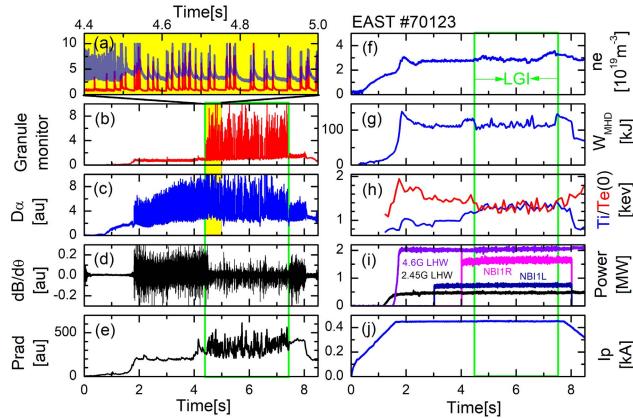

Fig. 7. Typical shot of ELM pacing by LGI during 4.4–7.4 s. (a) Granule monitor and ELM monitor by Dα signal. (b) Granule monitor by edge XUV signal. (c) Dα signal. (d) Magnetic perturbation. (e) Total radiation power from all XUV channels. (f) Line integrated plasma density. (g) Stored energy. (h) Core electron and ion temperature. (h) Heating scheme and injection power. (j) Plasma current.

envelope of triggered ELM is possibly due to the granule ablation before ELM burst. Irrespective of the confinement mode of the discharge, we note that the edge XUV signal appeared to be a relatively reliable indicator of granule penetration into the plasma.

IV. ELM PACING WITH LGI

Fig. 7 displays transiently successful ELM pacing by LGI. For this discussion, the term "ELM pacing" is used to describe the condition whereby nearly 100% of observed ELMs were triggered by LGI. The target discharges were run in an upper single-null configuration (shown in Fig. 1) with an ITER-like tungsten divertor. The total heating power applied is approximately 2.5 MW from lower hybrid heating and 2.3 MW neutral beam heating. Typical discharge parameters were as follows: $B_t = 2.6$ T, $I_P = 0.45$ MA, $W_{MHD} = 125$ kJ, and the ion grad-B drift was downward, away from the active divertor.

This discharge was in a naturally occurring high-frequency ELM regime of about 220 Hz. ELMs can be seen in Fig. 7(c), which shows the Dα traces. Granules were injected from $t = 4.4$–7.4 s, with an average velocity of $V_g \approx 75$ m/s and at an average injection rate of 99 Hz. The Li granule activity was indicated by edge XUV as shown in the granule monitor traces of Fig. 7(c). An expanded time window of the granule injection phase of the discharge is displayed in the first box in Fig. 7(b). It was found that after the first five granule injections, each subsequent granule was rapidly followed by an ELM. During the LGI phase, there is a strong correlation between the recorded ELMs and the granule injection events. Note that the ELM frequency is nearly equal to the granule injection frequency. The exception to this is a set of several clusters of small ELMs which occurred between two widely spaced granule injections. It was interesting to note that while the ELM frequency reduced by a factor of 2 the ELM amplitude did not increase by a commensurate amount. We conjecture that the first five granules lead to a long ELM-free period, and then each subsequent granule injection triggered an ELM. The ELM-pacing resulted in higher electron density, as shown in Fig. 7(f) where the line integrated density during the flat top was increased by 5%. Granule injection also resulted in a 15% lower stored energy.

V. SUMMARY AND FUTURE WORK

We report in this paper the first deployment of a multichamber LGI for ELM triggering experiments in EAST, using the upper divertor with tungsten PFCs. The upgraded capabilities from the first set of EAST experiments [11] performed well, allowing us to confirm the ability to trigger ELMs in a variety of conditions, and pace ELMs under select conditions.

Future experiments will focus on higher power discharges, and also discharges with a lower natural ELM frequency to determine if ELM amplitude varies inversely with triggered ELM frequency. In addition, experiments and analysis to determine why the present experiments showed modest confinement degradation, compared to DIII-D which showed no degradation under roughly similar conditions [10], are planned.

REFERENCES

[1] A. Loarte *et al.*, "Progress on the application of ELM control schemes to ITER scenarios from the non-active phase to DT operation," *Nucl. Fusion*, vol. 54, no. 3, p. 033007, 2014.

[2] R. Maingi, "Enhanced confinement scenarios without large edge localized modes in tokamaks: Control, performance, and extrapolability issues for ITER," *Nucl. Fusion*, vol. 54, no. 11, p. 114016, 2014.

[3] J. W. Connor, R. J. Hastie, H. R. Wilson, and R. L. Miller, "Magnetohydrodynamic stability of tokamak edge plasmas," *Phys. Plasmas*, vol. 5, no. 7, pp. 2687–2700, 1998.

[4] G. Federici *et al.*, "Effects of ELMs and disruptions on ITER divertor armour materials," *J. Nucl. Mater.*, vols. 337–339, pp. 684–690, Mar. 2005.

[5] L. R. Baylor *et al.*, "Reduction of edge-localized mode intensity using high-repetition-rate pellet injection in tokamak *H*-mode plasmas," *Phys. Rev. Lett.*, vol. 110, p. 245001, Jun. 2013.

[6] T. E. Evans *et al.*, "Edge stability and transport control with resonant magnetic perturbations in collisionless tokamak plasmas," *Nature Phys.*, vol. 2, pp. 419–423, May 2006.

[7] L. R. Baylor *et al.*, "ELM mitigation with pellet ELM triggering and implications for PFCs and plasma performance in ITER," *J. Nucl. Mater.*, vol. 463, pp. 104–108, Aug. 2015.

[8] P. T. Lang *et al.*, "ELM pacing and high-density operation using pellet injection in the ASDEX Upgrade all-metal-wall tokamak," *Nucl. Fusion*, vol. 54, no. 8, p. 083009, 2014.

[9] P. T. Lang *et al.*, "ELM pacing and trigger investigations at JET with the new ITER-like wall," *Nucl. Fusion*, vol. 53, no. 7, p. 073010, 2013.

[10] A. Bortolon *et al.*, "High frequency pacing of edge localized modes by injection of lithium granules in DIII-D H-mode discharges," *Nucl. Fusion*, vol. 56, no. 5, p. 056008, 2016.

[11] D. K. Mansfield *et al.*, "First observations of ELM triggering by injected lithium granules in EAST," *Nucl. Fusion*, vol. 53, no. 11, p. 113023, 2013.

[12] R. Lunsford *et al.*, "Lithium granule ablation and penetration during ELM pacing experiments at DIII-D," *Fusion Eng. Des.*, vol. 112, pp. 621–627, Nov. 2016.

[13] J. Li *et al.*, "A long-pulse high-confinement plasma regime in the experimental advanced superconducting tokamak," *Nature Phys.*, vol. 9, pp. 817–821, Nov. 2013.

Authors' photographs and biographies not available at the time of publication.